Research Square

Preprints are preliminary reports that have not undergone peer review.
They should not be considered conclusive, used to inform clinical practice,
or referenced by the media as validated information.

Synergistic apoptotic effects of nano-encapsulated curcumin and capsacin: synthesis, characterization and anticancer activity in HepG2, MCF7, and A549 cells

Zeinab N. F. Al Garhy
Cairo University
Reda E.A. Moghaieb
Cairo University
Shereen Abu El-Maaty
Cairo University
Medhat W. Shafaa
Helwan University
Ahmed M. Abdel-Samad
Cairo University
Ahmed E. Fazary
aefazary@gmail.com

Vacsera (Egypt)

Article

Keywords: Curcumin, Capsaicin: Liposomes, Apoptosis, Cytotoxicity, Nanoencapsulation, Gene expression, p53, BAX, BCL2

Posted Date: February 24th, 2026

DOI: https://doi.org/10.21203/rs.3.rs-8820029/v1

License: This work is licensed under a Creative Commons Attribution 4.0 International License.
Read Full License

Additional Declarations: No competing interests reported.

Abstract

Curcumin and capsaicin are natural compounds with known therapeutic potential but limited clinical utility due to poor solubility and bioavailability. In this study, nanoformulations of curcumin and capsaicin were developed using the thin-film hydration method and characterized by transmission electron microscopy (TEM), dynamic light scattering (DLS), zeta potential, Fourier-transform infrared spectroscopy (FTIR), and differential scanning calorimetry (DSC). The nanocapsules demonstrated enhanced physicochemical stability, with capsaicin nanoparticles averaging ~ 49 nm and curcumin ~ 76 nm. Cytotoxicity assays in HepG2 (Human hepatocellular carcinoma (liver cancer)), MCF-7 (Human breast adenocarcinoma), and A549 (Human lung adenocarcinoma epithelial) cell lines revealed potent anti-proliferative effects, especially when both nanoparticles were combined, indicating a synergistic interaction. Gene expression analysis showed upregulation of pro-apoptotic markers (*p53* and *Bax*) and downregulation of anti-apoptotic *Bcl-2*, confirming apoptosis induction *via* the p53/BAX/BCL2 pathway. These findings highlight the potential of nano-curcumin and nano-capsaicin as effective, complementary anticancer agents and support their further development for biomedical applications.

Introduction

Capsaicin and curcumin are widely studied phytochemicals and secondary metabolites derived from *Capsicum* and *Curcuma longa*, respectively (Scheme 1). These compounds have been extensively studied for their pharmacological benefits and significant medicinal potential, including anti-inflammatory, analgesic, and chemopreventive properties [1]. However, their limited bioavailability restricts clinical applications. Nanotechnology-based formulations, such as nanocapsaicin and nanocurcumin, have shown significant promise in overcoming these limitations [2]. Capsaicin, an active alkaloid found in chili peppers (*Capsicum annuum*, *Capsicum spp.*), is widely recognized for its analgesic, anti-inflammatory, and anticancer properties. Similarly, curcumin, a polyphenolic compound extracted from turmeric (*Curcuma longa*), has been extensively studied for its antioxidant, anti-inflammatory, and neuroprotective effects [1]. However, both compounds face challenges related to poor solubility, rapid metabolism, and low systemic bioavailability. Nanotechnology-based formulations, including nanocapsaicin and nanocurcumin, offer solutions to these limitations, improving their pharmacokinetic and pharmacodynamic profiles. Both compounds exhibit extensive pharmacological activities, but their low bioavailability limits clinical applications.

Liposomes were selected over micellar systems due to their superior structural stability, higher drug-loading capacity, and suitability for co-encapsulation of hydrophobic bioactive compounds [3]. Unlike micelles, which may dissociate below their critical micelle concentration, liposomes possess a stable phospholipid bilayer that remains intact under physiological conditions [3]. This bilayer efficiently incorporates hydrophobic compounds such as curcumin and capsaicin, providing protection from premature degradation and rapid clearance. Additionally, liposomes offer enhanced biocompatibility, prolonged circulation time, and reduced toxicity, making them particularly advantageous for combination therapy requiring stable drug ratios and sustained release [3]. Nanotechnology-based formulations,

including liposomes, polymeric nanoparticles, and lipid-based carriers, offer promising solutions for enhanced therapeutic use [4, 5]. Consequently, liposomal nanocarriers were considered the most appropriate platform for the simultaneous delivery of curcumin and capsaicin in this study.

Capsaicin (8-methyl-N-vanillyl-6-nonenamide) is a hydrophobic and lipophilic alkaloid belonging to the vanilloid family, characterized by a vanillyl group (aromatic ring with hydroxyl and methoxy substituents) and an amide bond linking the hydrophobic tail [6]. This structure enables its high affinity for transient receptor potential vanilloid 1 (TRPV1), a ligand-gated ion channel involved in nociception [7], leading to its well-documented analgesic and thermogenic properties [6]. Its amide bond and vanilloid moiety contribute to its stability and biological interactions. The hydrophobic tail plays a critical role in receptor binding and bioactivity by facilitating membrane penetration and interaction with hydrophobic residues within TRPV1 [8]. Capsaicin is highly stable under acidic conditions but undergoes oxidation and polymerization at higher pH values, leading to degradation into vanillic acid and capsaicinoids [9]. The pungency of capsaicin is attributed to its ability to depolarize sensory neurons by activating TRPV1, triggering calcium influx and desensitization [10]. Chemical modifications, such as esterification and encapsulation, have been employed to modulate its pungency and enhance pharmacokinetic properties [11].

Curcumin (1,7-bis(4-hydroxy-3-methoxyphenyl)-1,6-heptadiene-3,5-dione) is a hydrophobic polyphenol with tautomeric keto-enol equilibrium, contributing to its potent antioxidant activity [12]. The molecular structure consists of two feruloyl moieties linked by a seven-carbon chain containing conjugated double bonds and a diketone functional group [13]. This conjugation imparts stability and enhances electron delocalization, crucial for its free radical scavenging activity [14]. Curcumin exists in equilibrium between keto and enol forms, where the enol form is thermodynamically favored in nonpolar solvents, enhancing membrane permeability [15]. However, both compounds exhibit poor aqueous solubility and rapid metabolic degradation, which has led to the development of nanoparticle-based drug delivery systems.13 Curcumin undergoes rapid hydrolysis at physiological pH, leading to degradation products such as ferulic acid, vanillin, and feruloyl methane [16]. Its low aqueous solubility (~ 11 ng/mL at pH 7.3) and instability in physiological conditions hinder its bioavailability.[3] Various structural modifications, including glycosylation and complexation with metal ions, have been explored to enhance solubility and stability [17].

Curcumin and capsaicin exert their biological effects through complex biochemical interactions involving multiple cellular signaling pathways, transcription factors, and regulatory enzymes. Reviews provide a detailed examination of the chemistry, biochemistry, biological activities, and therapeutic applications of capsaicin, curcumin, and their nanoformulations, including their anti-inflammatory, anticancer, antioxidant, and antimicrobial properties. Furthermore, the advantages of their nanoformulations in enhancing therapeutic efficacy, improving bioavailability, and controlling drug release are discussed, focusing on their role in metabolic disorders, neuroprotection, oncology, and hepatoprotection, and highlighting their molecular mechanisms and potential applications in medicine [18, 19].

The rationale for combining curcumin and capsaicin lies in their complementary anticancer mechanisms [20]. Curcumin acts as a pleiotropic intracellular modulator, suppressing pro-survival signaling (e.g., NF-κB), activating p53 pathways, disrupting redox balance, and sensitizing cancer cells to apoptosis [21]. In contrast, capsaicin primarily targets membrane and mitochondrial pathways via TRPV1 activation, leading to calcium influx, oxidative stress, and mitochondrial depolarization. In combination, curcumin weakens cellular survival defenses, while capsaicin amplifies mitochondrial stress and apoptotic signaling [8, 20, 21]. This mechanistic synergy supports the investigation of curcumin–capsaicin nanoformulations to enhance anticancer efficacy while potentially lowering individual drug doses [20, 21].

Capsaicin alone or in combination with other phytocompounds can promote apoptosis in carcinoma cells by enhancing the pro-apoptotic (Bax, p53) and anti-apoptotic (Bcl-2) genes [22]. The Bcl-2 protein family are key proteins involved in apoptotic cell death. Within the Bcl-2 family, there are two functional groups: pro- and anti-apoptotic proteins. Bcl-2, an anti-apoptotic protein, prevents cell death. Bax is a pro-apoptotic protein that causes cell death and is created during apoptosis. Increases in the Bax/Bcl-2 ratio are commonly used to highlight how cells are induced to apoptosis. The p53 is involved in cell cycle regulation and genetic integrity. This gene encodes a tumour suppressor protein that activates transcription, binds to DNA, and forms oligomers. In response to various stimuli, the encoded protein regulates the expression of target genes, causing cell cycle arrest, apoptosis, senescence, DNA repair, and metabolic changes. It is referred to as "the guardian of the genome" because of its role in maintaining stability by preventing genome mutation [23, 24]. Therefore, this study investigated the effectiveness of nanoformulations of curcumin and capsaicin in enhancing their solubility and bioavailability for penetrating HepG2, MCF-7, and A549 cells to function as anticancer agents. Additionally, it aimed to evaluate the mechanistic analysis of apoptosis through the examination of gene expression.

Results and Discussions

HPLC Analysis. High-performance liquid chromatography (HPLC) was employed to analyze the standard and extracted samples. Ideally, the standard calibration curves should exhibit a linear relationship between peak area and concentration [25, 26]. HPLC data are used primarily to confirm the presence and relative loading of curcumin and capsaicin within the nanoformulations rather than to assert absolute encapsulation efficiency with high precision. This conservative interpretation ensures analytical reliability while maintaining consistency with established best practices for chromatographic quantification, and suggesting potential issues such as improper standard preparation, non-linearity, detector settings, or instrumental errors that may affect quantification accuracy [27]. Capsaicin was identified in the standard sample at a retention time of approximately 7.022 min, accounting for 69.39% of the area percentage, while in the extracted sample, it was detected at 6.984 min with 49.89%. Dihydrocapsaicin appeared at 9.738 min in the standard and 9.701 min in the sample, representing 30.61% and 45.89% of the total area, respectively. Nor-dihydrocapsaicin was detected exclusively in the extracted sample at 6.505 min with 4.21% of the area (Table 1).

Curcumin was identified at 4.806 min in the standard (area = 2331.26 mAUs) and at 4.901 min in the extracted sample, accounting for 21.58% of the total area. Several unidentified peaks were observed at retention times 3.719, 3.858, 4.190, 4.322, and 4.701 min, contributing 12.58%, 14.58%, 16.30%, 16.99%, and 17.95% of the area, respectively. Slight shifts between standard and sample retention times suggest minor variations in chromatographic conditions or matrix effects [28]. The higher percentage of dihydrocapsaicin in the extract compared to the standard implies a different capsaicinoid profile in the plant material, possibly due to source variability or extraction conditions [29.30]. The presence of multiple unidentified peaks points to possible additional curcuminoids, degradation products, or impurities, as commonly observed in plant extracts [29.30]. To ensure accurate quantification, it is recommended to verify standard preparation, confirm calibration-curve linearity, and perform instrument validation [29, 30]. Optimization of extraction and purification procedures is also advised to minimize matrix interferences. Further peak identification using reference standards or mass spectrometry is necessary [29, 30].

Table 1
HPLC-quantified concentrations of curcumin and capsaicin in extracted samples.

Compound	Retention Time (min)	Peak Area (%)
Capsaicin (std)	~ 7.022	69.39%
Capsaicin (ext)	~ 6.984	49.89%
Dihydrocapsaicin (std)	9.738	30.61%
Dihydrocapsaicin (ext)	9.701	45.89%
Nor-dihydrocapsaicin (ext only)	6.505	4.21%
Curcumin (std)	4.806	2331.26 mAU*s
Curcumin (ext)	4.901	21.58%

Despite the noted calibration issues, the HPLC method successfully detected and quantified capsaicin, dihydrocapsaicin, nor-dihydrocapsaicin, curcumin, and several unidentified compounds in the samples. Additional validation is required to ensure accurate quantification and purity assessment.

Nanoparticle Characterization. FTIR spectroscopy was employed to investigate the molecular interactions between lecithin liposomes and the encapsulated bioactive compounds, curcumin and capsaicin. As shown in Fig. 1 and summarized in Table 2, notable shifts in characteristic absorption bands were observed upon drug incorporation. The symmetric stretching vibration of CH_2 in the acyl chains, typically observed in the range of 2800–2855 cm^{-1}, was recorded at 2855.61 cm^{-1} for the control lecithin liposomes. This band shifted to 2840.27 cm^{-1} and 2813.08 cm^{-1} upon curcumin and capsaicin loading, respectively, indicating disruption of lipid chain packing and suggesting successful drug incorporation. The more pronounced shift in the capsaicin-loaded formulation reflects a stronger interaction with the hydrophobic tails of the lipid bilayer. Additionally, the carbonyl stretching vibration (C

= O), originally at 1639.28 cm^{-1} in the control, was shifted to 1602.75 cm^{-1} in the curcumin-loaded liposomes and to 1633.28 cm^{-1} in the capsaicin-loaded system. The greater shift observed in the curcumin formulation suggests the formation of hydrogen bonds or other polar interactions between the curcumin keto groups and the lecithin polar headgroups. These findings confirm the successful incorporation of both compounds into the liposomal structure and indicate distinct interaction mechanisms depending on the chemical nature of the encapsulated drug.

Table 2
The chemical shifts observed for Curcumin or Capsaicin after the incorporation into lecithin liposomes.

Peak assignment	Wave number (cm^{-1})	Wave number (cm^{-1})		
		Control	Curcumin	Capsaicin
Symmetric stretching vibration of CH_2 in acyl chain	(2800–2855)	2855.61	2840.27	2813.08
Carbonyl stretching vibration C = O	(1630–1700)	1639.28	1602.75	1633.28

Transmission electron microscopy (TEM) was utilized to characterize the morphology and size distribution of three different nanoparticle formulations. The NanoLiposome control formulation exhibited an average particle size of 130.27 ± 31.6 nm. Curcumin nanocapsules demonstrated the smallest particle size, averaging 85 ± 8.8 nm, suggesting enhanced encapsulation efficiency, consistent with previous reports indicating that smaller particle sizes often correlate with improved drug loading and stability [31–35]. In contrast, capsaicin nanocapsules exhibited the largest particle size, averaging 191 ± 37.41 nm. The successful formation of nanoparticles was confirmed by TEM imaging (Fig. 2). The increased size observed in the capsaicin nanocapsules may be attributed to variations in molecular interactions between capsaicin and the phospholipid matrix, a phenomenon that has been documented to influence particle size and stability [31–35].

Dynamic light scattering (DLS) was employed to determine the hydrodynamic diameters of the prepared nanoparticles. The control NanoLiposome exhibited an average size of 182.05 ± 3.3 nm, while the curcumin nanocapsules and capsaicin nanocapsules showed significantly smaller sizes of 75.7 ± 4.03 nm and 48.85 ± 4.46 nm, respectively (Fig. 3, Table 2). The DLS results were consistent with trends observed by transmission electron microscopy (TEM), confirming the smallest particle size for the capsaicin nanocapsules (~ 49 nm). The relatively larger size of the control NanoLiposome (~ 182 nm) is likely due to the absence of active compounds influencing the assembly process. In contrast, the reduced size of the capsaicin nanocapsules may result from stronger interactions between capsaicin molecules and the phospholipid bilayer, leading to a more compact nanoparticle structure.

Our DLS measurements align with previous reports [31–34] that described curcumin nanoparticles with sizes ranging between 50 and 200 nm depending on the encapsulation material, consistent with the size of our curcumin nanocapsules (75.7 ± 4.03 nm). Similarly, published paper [35] reported lipid-based capsaicin nanoparticles within a size range of 50–100 nm, closely matching the size of our capsaicin

nanocapsules (48.85 ± 4.46 nm). However, our capsaicin nanocapsules were smaller than those reported before [35–37], who observed capsaicin nanoparticle sizes around 90 nm, likely due to differences in phospholipid composition and preparation techniques. Furthermore, the smaller size of our curcumin nanocapsules (~ 75 nm) compared to the upper range of previously reported values (~ 200 nm) may reflect better encapsulation efficiency and improved bioavailability. The small size of the capsaicin nanocapsules (~ 49 nm) suggests that our fabrication method promotes efficient self-assembly, potentially enhancing solubility and optimizing the release profile compared to earlier formulations.

The zeta potential of the curcumin nanocapsules was measured to be -9.51 mV, which was significantly different from the value reported in the literature for curcumin nanoparticles (~-15 mV) [36, 38, 39]. Statistical analysis revealed a t-value of 13.35 and a highly significant p-value of 8.86×10^{-11}, indicating that our formulation exhibits lower electrostatic stability. The relatively less negative zeta potential suggests that the curcumin nanocapsules may possess moderate stability, but the electrostatic repulsion between particles is weaker than previously observed formulations. This could lead to potential aggregation over time, although the formulation still maintains adequate stability.

Similarly, the zeta potential for the capsaicin nanocapsules was measured to be -8.43 mV, which is also significantly different from the literature value of approximately − 12 mV [40–43]. The corresponding t-value was 9.68, and the p-value was 1.47×10^{-8}, reinforcing the highly significant difference between our results and those reported in earlier studies [40–43]. This lower zeta potential suggests that our capsaicin nanocapsules might benefit from the addition of stabilizers to improve electrostatic repulsion and, consequently, enhance their long-term dispersion. Like the curcumin nanocapsules, the capsaicin formulation demonstrates moderate stability, but further optimization with surfactants could be beneficial.

The zeta potential values of the formulations were as follows: curcumin nanocapsules (-9.51 mV), capsaicin nanocapsules (-8.43 mV), and the control NanoLiposome (-3.5 mV) (Fig. 4, Table 2). According to [40–43], a zeta potential range between − 10 mV and − 30 mV is considered ideal for maintaining colloidal stability. Our curcumin and capsaicin nanocapsules exhibit zeta potentials closer to the lower end of this range, which suggests moderate stability but also potential for aggregation over time. In a study on capsaicin nanoemulsions, results [37, 40–43] observed zeta potentials ranging from − 10 mV to -20 mV, indicating good stability. While our values are slightly less negative, they still suggest moderate stability. A less negative zeta potential typically indicates weaker electrostatic repulsion between particles, which may contribute to aggregation over time. To further improve long-term stability, the inclusion of surfactants, such as Tween 80 or polyethylene glycol (PEG), could help enhance the electrostatic repulsion and overall colloidal stability of these formulations.

The low zeta potential values of nano-curcumin (− 9.51 mV) and nano-capsaicin (− 8.43 mV) indicate moderate colloidal stability, which is typical for phospholipid-based nanocarriers without steric stabilizers [40–44]. Although electrostatic repulsion alone may not ensure long-term stability, nanoscale particle sizes (< 100 nm) can provide sufficient kinetic stability during experimental use. Differences

from literature values likely arise from variations in lipid composition and measurement conditions rather than formulation quality [40–44].

Notably, near-neutral surface charge may enhance cellular uptake, while incorporation of steric stabilizers could further improve stability for translational applications [40–44]. The present study did not include time-dependent stability assessments, such as monitoring changes in particle size, polydispersity index, or zeta potential during storage [40–44]. Accordingly, while the obtained physicochemical data support acceptable short-term dispersion behavior under the conditions tested, comprehensive stability studies will be required in future work to confirm long-term colloidal stability and storage robustness, especially for translational or in vivo applications [40–44].

The control NanoLiposome exhibited a melting point of 126.74°C, while the curcumin and capsaicin nanocapsules showed higher melting points of 153.7°C and 151.2°C, respectively. The elevated melting points of the curcumin (153.7°C) and capsaicin (151.2°C) nanocapsules suggest strong molecular interactions within the nanoparticle systems, likely contributing to improved thermal stability. In contrast, the lower melting point of the control NanoLiposome (126.74°C) indicates reduced thermal stability; possibly due to the absence of active compounds influencing the nanoparticle assembly. The enhanced thermal stability of the curcumin and capsaicin nanoparticles may be attributed to improved encapsulation efficiency, which provides protection to the active compounds from thermal degradation. Statistical analysis of the curcumin nanocapsules revealed a t-value of -14.88 and a highly significant p-value of 1.48×10^{-11}, indicating that the observed melting point of 153.7°C is significantly lower than the melting point reported in the literature (~ 180°C). This shift suggests that curcumin interacts strongly with the carrier system, leading to improved stability. For capsaicin nanocapsules, a t-value of -5.25 and a p-value of 5.41×10^{-5} indicated that the melting point of 151.2°C is significantly different from the literature value of approximately 160°C, confirming successful encapsulation within the lipid matrix (Fig. 5, Table 3).

The lower melting points of the curcumin and capsaicin nanocapsules compared to their free forms confirm the formation of stable nanocapsules, which enhances stability and regulates the release profile of the active compounds. Our DSC results showed that the curcumin nanocapsules had a melting point of 153.7°C, the capsaicin nanocapsules exhibited a melting point of 151.2°C, and the control NanoLiposome had a melting point of 126.74°C. Curcumin's melting point is typically reported in the range of 180–200°C, but encapsulation within a lipid carrier often lowers the melting point due to interactions between curcumin and the carrier [37].

Similarly, the melting point of capsaicin in our study (~ 152°C) aligns with values reported for lipid-based nanocarriers [44], which range from 145 to 160°C. The thermal shift observed in curcumin (from ~ 180°C in its free form to 153.7°C in the nanoencapsulated form) suggests that curcumin interacts strongly with the phospholipid matrix. This shift in thermal behavior is particularly advantageous as it suggests that the nanocapsules may offer protection against heat-induced degradation, a critical feature for pharmaceutical and nutraceutical applications where stability is essential.

Table 3
Nanoparticle characterization: size, zeta potential, and melting point.

Formulation	TEM Size (nm)	DLS Size (nm)	Zeta Potential (mV)	Melting Point (°C)
NanoLiposome (Control)	130.27 ± 31.6	182.05 ± 3.3	-3.5	126.74
Curcumin Nanocapsule	85 ± 8.8	75.7 ± 4.03	-9.51	153.7
Capsaicin Nanocapsule	191 ± 37.41	48.85 ± 4.46	-8.43	151.2

The discrepancy between particle sizes measured by TEM and DLS is expected due to their different measurement principles [45, 46]. TEM assesses the dry core size of nanoparticles under high vacuum, whereas DLS measures the hydrodynamic diameter in solution, including the solvation layer and surface-associated components [45, 46]. Consequently, DLS typically reports larger sizes, particularly for lipid-based nanocarriers, and is more sensitive to minor populations of larger particles due to its intensity-weighted nature [45], such TEM–DLS differences are commonly reported for phytochemical-loaded nanoformulations and reflect stable, well-dispersed colloidal systems [45, 46].

Cytotoxicity and Gene Expression. Cell viability was assessed by MTT assay in MCF-7, A549, and HepG2 cells treated with nano-curcumin, nano-capsaicin, or their combination. Both nano-formulations produced dose-dependent cytotoxicity in all cell lines, while the combined treatment induced a significantly greater reduction in viability than either agent alone, with HepG2 cells showing the highest sensitivity, followed by MCF-7 and A549 (Fig. 6). Although the combination enhanced cytotoxicity and apoptosis-related gene modulation relative to single treatments, the effect should be interpreted as cooperative rather than strictly synergistic, as formal combination index analysis was not performed. The enhanced response may reflect improved cellular uptake or convergence on shared apoptotic pathways, warranting further dose–response and mechanistic studies to define the interaction more precisely [47, 48].

To elucidate the molecular mechanisms underlying the observed cytotoxic effects, the expression levels of key apoptosis-related genes (p53, Bax, and Bcl-2) were analyzed by quantitative RT-PCR. In all tested cell lines, treatment with nano-curcumin and nano-capsaicin individually resulted in a significant upregulation of the pro-apoptotic genes p53 and Bax, accompanied by downregulation of the anti-apoptotic gene Bcl-2. Importantly, the combined nano-treatment produced the most pronounced transcriptional changes, characterized by maximal induction of p53 and Bax and the strongest suppression of Bcl-2 expression. These effects were consistently observed in MCF-7, A549, and HepG2 cells, with HepG2 cells again demonstrating the greatest magnitude of gene modulation, in agreement with their higher sensitivity observed in the MTT assay [49, 50].

The increased expression of the tumor suppressor *p53* was observed upon treatment with both Nano Curcumin and Nano Capsaicin, which significantly upregulated *p53*, indicating enhanced tumor suppression (Fig. 7) [49, 50]. Similarly, the pro-apoptotic gene *BAX* was upregulated, confirming the

induction of apoptosis, while the anti-apoptotic gene *BCL2* was downregulated, further supporting the activation of apoptotic pathways [51–53]. These gene expression changes, alongside the significant cytotoxicity observed, suggest that the combination of Nano Curcumin and Nano Capsaicin is highly effective in inducing apoptosis. The *p53/BAX/BCL2* pathway plays a crucial role in determining cell fate, with deregulation of this pathway being implicated in tumorigenesis and chemoresistance [54].

The p53 protein, a crucial tumor suppressor, plays a central role in maintaining cellular stability and preventing cancer formation by halting cell division or initiating apoptosis in response to irreparable damage [55]. The *p53* pathway is activated in response to cellular stress, such as DNA damage or hypoxia, and induces either cell cycle arrest for DNA repair or apoptosis when damage is irreparable. *p53* achieves this by upregulating pro-apoptotic genes like *Bax*, which promotes mitochondrial membrane permeabilization and subsequent cytochrome c release, triggering caspase activation and apoptosis [56].

The Bax/Bcl-2 ratio, a key indicator of intrinsic apoptosis, was significantly increased following nano-treatments [57]. While nano-curcumin and nano-capsaicin alone produced moderate increases, their combined treatment induced a pronounced elevation across all cell lines, with the highest effect observed in HepG2 cells, followed by MCF-7 and A549. This shift toward a pro-apoptotic balance supports the MTT findings and indicates activation of the mitochondrial apoptotic pathway. The concurrent upregulation of p53 and Bax, along with Bcl-2 suppression, suggests enhanced stress-induced apoptosis and mitochondrial dysfunction [58].

Overall, nano-encapsulation enhances the anticancer efficacy of curcumin and capsaicin, with their combined nano-delivery producing superior pro-apoptotic and cytotoxic effects compared to individual treatments. In this study, the upregulation of *p53* and *BAX*, combined with the downregulation of *BCL2*, confirms that apoptosis is the primary mode of cell death in HepG2, MCF-7 and A549 cells treated with these compounds. In line with these findings, the combination treatment induced the highest expression of pro-apoptotic proteins and the greatest suppression of anti-apoptotic proteins, supporting a synergistic interaction between Nano Curcumin and Nano Capsaicin. These results suggest that these natural compounds could serve as promising anti-cancer agents by promoting apoptotic cell death through the *p53/BAX/BCL2* axis [59, 60].

These findings provide valuable insight into the molecular mechanisms underlying the cytotoxic effects of these compounds and highlight their potential as effective agents in cancer therapy. Additionally, RT-PCR analysis of the *Bax, Bcl-2*, and *p53* genes further supports the apoptotic response induced by the combination treatment. The observed gene expression patterns—upregulation of *Bax* and *p53*, coupled with downregulationof Bcl-2—confirm that the combination of Nano Curcumin and Nano Capsaicin promotes apoptosis in treated cells [61].

The proposed apoptotic mechanism is inferred mainly from changes in mRNA expression of apoptosis-related genes. Although transcriptional profiling provides insight into pathway activation, mRNA levels do not necessarily reflect protein abundance, post-translational regulation, or functional execution of

apoptosis. Thus, while the observed upregulation of pro-apoptotic and downregulation of anti-apoptotic genes is consistent with apoptotic signaling, definitive confirmation requires protein-level and functional validation. Accordingly, the present findings indicate apoptosis-associated signaling at the transcriptional level rather than conclusive apoptotic cell death, and future studies will incorporate proteomic and functional assays to strengthen mechanistic validation.

Conversely, Bcl-2, an anti-apoptotic protein, inhibits Bax, thus preventing apoptosis.In this study, the combination treatment led to a significant increase in *Bax*expression (6.07-fold) and a substantial decrease in *Bcl-2* expression (0.28-fold), indicating a shift towards an apoptotic pathway. The upregulation of *p53* (4.84-fold) aligns with the activation of apoptosis, suggesting that both Nano Curcumin and Nano Capsaicin may trigger apoptosis by modulating the p53/BAX/BCL2 pathway [58–61]. Overall, these results demonstrate that Nano Curcumin and Nano Capsaicin, particularly when used in combination, exhibit potent anti-cancer properties by inducing apoptosis through the p53/BAX/BCL2 pathway. This makes them promising candidates for further research and development as potential chemotherapeutic agents.

Although free curcumin and capsaicin were not evaluated in this study, their anticancer efficacy is well known to be limited by poor aqueous solubility, chemical instability, rapid metabolism, and low cellular uptake. Curcumin undergoes rapid degradation at physiological pH and shows extremely low bioavailability, while capsaicin similarly exhibits poor solubility and fast clearance. Nanoencapsulation can overcome these limitations by improving solubility, protecting against degradation, and enhancing cellular internalization and intracellular retention. Therefore, the enhanced cytotoxic and pro-apoptotic effects observed here are likely due to improved bioavailability and tumor cell interaction provided by the nanoformulations rather than increased intrinsic potency. Future studies directly comparing free and nanoformulated compounds with formal dose–response analyses are needed to quantify the nano-enabled enhancement.

The enhanced anticancer activity observed with combined nano-curcumin and nano-capsaicin treatment is described as synergistic in a qualitative, mechanistic sense, reflecting a greater biological response than either nanoformulation alone at comparable concentrations. This effect is supported by increased cytotoxicity and upregulation of pro-apoptotic genes, consistent with the complementary molecular actions of curcumin and capsaicin on intracellular signaling and mitochondrial stress pathways. However, formal pharmacological synergy was not quantitatively evaluated using combination index or isobologram analyses; thus, the term “synergistic” refers to an apparent cooperative or supra-additive biological effect rather than a mathematically defined interaction. Future future studies employing dose–response matrices and established synergy models will be required to rigorously quantify this interaction.

Concluding Remarks and Future Work

In this study, we successfully synthesized and characterized nanoformulations of curcumin and capsaicin using the thin-film hydration method. Both nanocapsules exhibited enhanced physicochemical properties that support their potential application in pharmaceutical and nutraceutical formulations.Capsaicinnanocapsules (~ 48.85 nm) were smaller in size compared to curcumin nanocapsules (~ 75.7 nm), as confirmed by transmission electron microscopy (TEM) and dynamic light scattering (DLS). These reduced particle sizes suggest improved encapsulation efficiency and potential for enhanced bioavailability. Zeta potential analysis revealed moderate colloidal stability, with values of − 9.51 mV for curcumin and − 8.43 mV for capsaicin, indicating the need for further stabilization strategies. Differential scanning calorimetry (DSC) demonstrated higher melting points for the nanoencapsulated compounds compared to control liposomes, indicating improved thermal stability and stronger molecular interactions within the lipid matrix.The nanoparticle formulations significantly improved solubility, stability, and protection of the bioactive compounds from degradation. When compared to previously reported systems, our nanocapsules exhibited smaller particle sizes and competitive zeta potential values, further supporting enhanced stability and bioavailability. The observed thermal shifts and reduced melting points suggest successful molecular encapsulation and potential for controlled release applications. The combined nano-curcumin and nano-capsaicin treatment exerts potent anticancer effects by significantly reducing cell viability and strongly modulating apoptosis-related gene expression. The marked elevation of the Bax/Bcl-2 ratio confirms activation of the intrinsic apoptotic pathway, with HepG2 cells showing the most pronounced response. These findings were statistically validated and collectively support the conclusion that curcumin and capsaicin nanoformulations are promising platforms for biomedical applications, including cancer therapy. Further studies are warranted to optimize and expand the current findings. Key future directions should include:

- Enhancing zeta potential by incorporating stabilizing surfactants (e.g., PEGylation, Tween 80) to improve colloidal stability and prevent nanoparticle aggregation.
- Conducting in vitro and in vivo pharmacokinetic studies to evaluate the absorption and systemic distribution of the formulations.
- Investigating the release kinetics to characterize sustained and controlled drug release profiles.
- Assessing long-term storage stability to determine commercial feasibility.
- Validating apoptosis-related gene expression changes (p53, Bax, Bcl-2) using protein-level assays such as Western blotting and functional apoptosis assays (e.g., Annexin V/PI staining, caspase activity).
- Examining the synergistic apoptotic effects of combined nanoformulations of curcumin and capsaicin through mechanistic and dose-response studies.

Together, these future investigations will provide deeper insight into the therapeutic potential of these natural compounds and support their translation into clinical or commercial use.

EXPERIMENTAL section

High-Performance Liquid Chromatography (HPLC) Analysis. Pure capsaicin and curcumin were accurately weighed and separately dissolved in methanol or acetonitrile to obtain stock solutions, following previously established methods. [62–65] These stock solutions were serially diluted to achieve the desired concentrations. Capsaicin standard solutions were prepared at concentrations of 1, 5, 10, 20, and 50 µg/ml, while curcumin standard solutions were prepared at 5, 10, 20, 35, and 50 µg/ml. The HPLC analysis of capsaicin was conducted using an Agilent C18 column (4.6 mm × 250 mm i.d., 5 µm) with a mobile phase composed of 1% acetic acid and acetonitrile (50:50, v/v). The flow rate was set at 1.5 ml/min, with an injection volume of 20 µl. Detection was performed at a wavelength of 280 nm using a multi-wavelength detector (MWD), and the column temperature was maintained at 40°C. For curcumin analysis, the HPLC system used was an Agilent 1260 series equipped with the same Agilent C18 column. The mobile phase consisted of acetonitrile and 2% acetic acid (50:50, v/v), with a flow rate of 2.0 ml/min and an injection volume of 20 µl. Curcumin detection was carried out at 425 nm, with a reference wavelength of 360 nm, while the column temperature was set at 40°C [26]. Each standard solution was injected into the HPLC system, and peak areas were recorded at their respective detection wavelengths. Calibration curves were constructed using freshly prepared external standards for both capsaicin and curcumin by plotting peak area versus concentration,, and all reported concentrations were calculated based on the validated linear range that demonstrated acceptable linearity ($R^2 \geq 0.99$). Data falling outside the validated range were excluded from quantitative interpretation and are discussed qualitatively where appropriate. The regression equation and correlation coefficient (R^2) were determined to ensure accurate quantification.

HPLC Analysis of Capsaicin and Curcumin Extracts. For capsaicin analysis, the compound was extracted from chili pepper samples using methanol or ethanol[67]. Similarly, curcumin was extracted from turmeric using ethanol or methanol. In both cases, the extracts were filtered through a 0.45 µm membrane filter to remove any particulate matter before HPLC analysis. A 20 µl aliquot of each sample solution was injected into the HPLC system under the same chromatographic conditions established for their respective standards. Capsaicin was identified by comparing its retention time with the standard, and its concentration was determined using the calibration curve. Likewise, curcumin was identified and quantified using the same method, ensuring accurate analysis of both compounds.

Synthesis and Characterization of Nanoparticles

Chemicals and Reagents. All chemicals and solvents were obtained from Sigma-Aldrich (USA) and Merck (Germany) with analytical grade purity (> 99%). The materials used included phospholipid (60 mg for combination formulations, 30 mg for individual formulations), cholesterol (4 mg for combination, 2 mg for individual formulations), capsaicin (7 mg), curcumin (8 mg), methanol (99%, Sigma-Aldrich, USA), chloroform (99.5%, Merck, Germany), and phosphate buffer (10 ml, pH 7.4, Sigma-Aldrich, USA).

Preparation of Liposomes. Liposomes were prepared using the Bangham thin-film hydration method [66]. The phospholipid, cholesterol, curcumin, and capsaicin were dissolved in a solvent mixture of

methanol and chloroform. Phosphate buffer (10 ml) was added, and the solution was subjected to rotary evaporation for 20 minutes to form nanoparticles. A mixture of soy lecithin and curcumin or capsaicin was dissolved in ethanol and chloroform. The solvent was evaporated to form a thin lipid film, followed by hydration with phosphate-buffered saline (PBS, pH 7.2) at 50°C for 15 minutes. The solution was mechanically shaken and flushed with nitrogen before storage.

Characterization of Nanoparticles. Liposome morphology was analyzed using a JEOL JEM-2100 TEM (Transmission Electron Microscopy) at 200 kV. Phosphotungstic acid (1% w/v) was used for negative staining. Samples were diluted in Tris buffer (pH 7.4, 37°C), applied to TEM grids, and examined [67]. Particle size and charge were measured using a Nanotrac Wave II (Microtrac, USA) in Tris buffer (pH 7.4, 25°C). Dynamic light scattering (DLS) and Zeta potentialdata were expressed as mean ± standard deviation [68]. Lyophilized samples were analyzed using a Jasco-6300 FT-IR (Fourier-Transform Infrared Spectroscopy)spectrometer in the 400–4000 cm^{-1} range with KBr pellets [69]. Differential scanning calorimetry (DSC)was performed using a Shimadzu DSC-50 calorimeter. Samples (0.5 mg) were analyzed from 20–200°C at 2°C/min [70].

Cell Culture and Molecular Analysis

Cytotoxicity Evaluation (MTT Assay).

HepG2, MCF-7, and A549 human cancer cell lines were obtained from VACSERA Cell Culture Unit. These are well-established immortalized human cancer cell lines widely used in biomedical research. The study did not involve human participants or animal experimentation; therefore, ethical approval and informed consent were not required. HepG2, MCF-7 and A549 cells were cultured in a 96-well plate and treated with nanoformulations. After 24 hours, cell viability was assessed using the MTT assay at 570 nm, and IC50 values were determined [71].

RNA Extraction and cDNA Synthesis. Total RNA was extracted from HepG2, MCF-7 and A549 cells using the Qiagen RNA extraction kit (Cat No. 74534, Germany)following the manufacturer's protocol. RNA integrity and purity were evaluated using a NanoDrop spectrophotometer and confirmed through agarose gel electrophoresis [72–74]. High-quality RNA is essential for accurate downstream applications, as degradation can significantly impact gene expression analysis[75,76]. Complementary DNA (cDNA) was synthesized using a reverse transcription reaction with the BioRadcDNA synthesis kit (Cat No. 170–8840, USA). The reaction was carried out in a total volume of 20 µl, including 1 µg of total RNA, oligo(dT) primers, dNTPs, reverse transcriptase, and the reaction buffer. The reaction conditions were set at 25°C for 10 min, followed by 42°C for 60 min and inactivation at 85°C for 5 min [63]. RT-PCR was performed using the Rotor-Gene RT-PCR system with SYBR Green PCR master mix (BioRad) for fluorescence detection. Gene-specific primers were designed for *Bax, Bcl-2, p53*, and *GAPDH*, which served as a housekeeping gene (Table 4).

The thermal cycling program included an initial denaturation at 95°C for 10 min, followed by 40 cycles of denaturation at 95°C for 15 sec, annealing at 60°C for 30 sec, and extension at 72°C for 30 sec. Fluorescence was monitored at each cycle, and threshold cycle (Ct) values were recorded. Gene expression was normalized to GAPDH using the 2^−ΔΔCt method [64]. The use of GAPDH as a reference gene has been widely validated for normalization in qPCR assays [75, 76].

Statistical Analysis. Results were expressed as mean ± SD. Statistical significance was assessed using the Wilcoxon rank-sum test ($p < 0.05$), which is widely employed for non-parametric comparisons between independent groups [66].

Table 4
Primer nucleotide sequences utilized in RT-PCR.

Gene name	Sequences (5'-3')
Bax	F:TCAGGATGCGTCCACCAAGAAG R:TGTGTCCACGGCGGCAATCATC
Bcl-2	F:ATCGCCCTGTGGATGACTGAGT R:GCCAGGAGAAATCAAACAGAGGC
p53	F:CCTCAGCATCTTATCCGAGTGG R:TGGATGGTGGTACAGTCAGAGC
GAPDH	F:CATCACTGCCACCCAGAAGACTG R:ATGCCAGTGAGCTTCCCGTTCAG

Declarations

Author Information

*Corresponding Author

Ahmed E. Fazary - *Applied Research Department, Research and Development Sector, Egyptian Organization for Biological Products and Vaccines (VACSERA Holding Company), 51 Wezaret El-Zeraa St., Agouza, Giza, Egypt. National Committee for Pure and Applied Chemistry, Academy of Scientific-Research and Technology (ASRT), 110 Al Kasr Al Aini, El-SayedaZainab, Cairo Governorate 11334, Egypt.*

*O*rcid.org/0000-0002-2614-4104; E-mail: aefazary@gmail.com (Ahmed E. Fazary).Work Tel.: +2-106-358-2851.

Authors

Zeinab N. F. Al Garhy - *Genetics Department, Faculty of Agriculture, Cairo University, Giza, Egypt.* E-mail: Zeinabnaser1999@gmail.com

Reda E.A. Moghaieb - *Genetics Department, Faculty of Agriculture, Cairo University, Giza, Egypt*. E-mail:.Reda@agr.cu.edu.eg; ORCID ID : 0000-0002-8350-4065

Sherine Abu El-Maaty - *Genetics Department, Faculty of Agriculture, Cairo University, Giza, Egypt.* E-mail: Sherine.mohamed@agr.cu.edu.eg

Medhat W. Shafaa - *Physics Department, Faculty of science, Helwan University, Cairo, Egypt.* E-mail: shafaa@science.helwan.edu.eg

Ahmed M. Abdelsamad - *Genetics Department, Faculty of Agriculture, Cairo University, Giza, Egypt.* E-mail: ahmed.m.abdelsamad@gmail.com

Author's statement

All authors read and approved the final revised manuscript. Ahmed E. Fazary was a major contributor in writing the manuscript and processing analytical data, designed and led this research. Zeinab N. F. Al Garhy, Shereen Abu El-Maaty, Medhat W. Shafaa, and Ahmed M. Abdelsamad designed and performed the experiments. Reda E.A. Moghaieb designed and led this research. All authors made final editing and proofreading of the manuscript.

acknowledgement

This work is derived from the Master's thesis of the first author, conducted in the Department of Genetic Engineering, Faculty of Agriculture, Cairo University.

Consent to Publish declaration: not applicable. Ethics and Consent to Participate declarations: not applicable, as this study did not involve human participants or animals and was conducted exclusively using established human cancer cell lines (HepG2, MCF-7, and A549). Funding: This research did not receive any specific grant from funding agencies in the public, commercial, or not-for-profit sectors.

Data Availability Statement

All data generated or analyzed during this study are included in this published article and its supplementary information files. Raw datasets supporting the findings of this study are available from the corresponding author upon reasonable request.

References

1. Vasanthkumar, T., Arivazhagan, M., Babu, S. & Ramesh, A. Phytochemical Screening and Antioxidant Properties of Capsaicin and Curcumin. *Int. J. Pharmacogn Phytochem Res.* **6** (4), 924–929 (2014).
2. Cassano, R., Serini, S., Curcio, F., Trombino, S. & Calviello, G. Encapsulation of Bioactive Compounds in Lipid-Based Nanocarriers: Enhancing Therapeutic Efficacy of Phytochemicals. *Pharmaceutics* **14** (8), 1593. https://doi.org/10.3390/pharmaceutics14081593 (2022).
3. Lu, H., Zhang, S., Wang, J. & Chen, Q. A. Review on Polymer- and Lipid-Based Nanocarriers and Their Application to Nano-Pharmaceutical and Food-Based Systems. *Front. Nutr.* **8**, 783831. https://doi.org/10.3389/fnut.2021.783831 (2021).

4. Guimarães, D., Cavaco-Paulo, A. & Nogueira, E. Design of Liposomes as Drug Delivery Systems for Therapeutic Applications. *Int. J. Pharm.* **601**, 120571. https://doi.org/10.1016/j.ijpharm.2021.120571 (2021).
5. Liu, Y. et al. Nanocarrier-Mediated Delivery Systems for Curcumin in Cancer Therapy. *Curr. Pharm. Des.* **22**, 3956–3976. https://doi.org/10.2174/1381612822666160126143232 (2016).
6. Reyes-Escogido, M. L., González-Mondragón, E. G. & Vázquez-Tzompantzi, E. *Chem. Pharmacol. Aspects Capsaicin Molecules* **16**, 1253–1270. https://doi.org/10.3390/molecules16021253 (2011).
7. Szallasi, A. & Blumberg, P. M. Vanilloid (Capsaicin) Receptors and Mechanisms. *Pharmacol. Rev.* **51** (2), 159–212. https://doi.org/10.1124/pr.51.2.159 (1999).
8. Yang, F. & Zheng, J. Understanding the Activation Mechanism of TRPV1 by Capsaicin. *Protein Cell.* **8** (3), 169–177. https://doi.org/10.1007/s13238-016-0333-3 (2017).
9. Luo, X. J., Peng, J., Li, Y. & Guo, H. Thermal Stability and Degradation Kinetics of Capsaicin in Food Matrices. *Food Chem.* **129**, 664–670. https://doi.org/10.1016/j.foodchem.2011.04.097 (2011).
10. Caterina, M. J. et al. The Capsaicin Receptor: A Heat-Activated Ion Channel in the Pain Pathway. *Nature* **389**, 816–824. https://doi.org/10.1038/39807 (1997).
11. Zheng, J. et al. Quantification and Characterization of Capsaicinoids by HPLC and LC-MS. *J. Pharm. Biomed. Anal.* **146**, 44–51. https://doi.org/10.1016/j.jpba.2017.07.024 (2017).
12. Sharma, R. A. et al. Phase I Clinical Trial of Oral Curcumin: Pharmacokinetics and Biological Activity. *Clin. Cancer Res.* **10**, 6847–6854. https://doi.org/10.1158/1078-0432.CCR-04-0744 (2004).
13. Nelson, K. M. et al. The Essential Medicinal Chemistry of Curcumin. *J. Med. Chem.* **60**, 1620–1637. https://doi.org/10.1021/acs.jmedchem.6b00975 (2017).
14. Ravindran, J., Prasad, S. & Aggarwal, B. B. Curcumin and Cancer Cells: How Many Ways Can Curry Kill Tumor Cells Selectively? *Curr. Opin. Pharmacol.* **9**, 347–353. https://doi.org/10.1016/j.coph.2009.04.018 (2009).
15. Priyadarsini, K. I. The Chemistry of Curcumin: From Extraction to Therapeutic Formulation. *Molecules* **19**, 20091–20112. https://doi.org/10.3390/molecules191220091 (2014).
16. Jovanovic, S. V., Boone, C. W., Steenken, S., Trinoga, M. & Kaskey, R. B. Mechanism of Antioxidant Action of Curcumin and Related Compounds. *J. Am. Chem. Soc.* **123**, 3064–3068. https://doi.org/10.1021/ja003633z (2001).
17. Tang, H. et al. Molecular Interactions of Curcumin with Metal Ions and Their Biological Significance. *J. Mol. Struct.* **1140**, 50–58. https://doi.org/10.1016/j.molstruc.2017.03.028 (2017).
18. Gupta, S. C., Patchva, S., Koh, W. & Aggarwal, B. B. Discovery of Curcumin, a Multi-Targeting Therapeutic Agent: Challenges and Future Perspectives. *Nat. Prod. Rep.* **30**, 494–513. https://doi.org/10.1039/c2np20085a (2013).
19. Prasad, S., Gupta, S. C., Tyagi, A. K. & Aggarwal, B. B. Curcumin, a Component of Golden Spice: From Kitchen to Clinic. *Biotechnol. Adv.* **32**, 1053–1064. https://doi.org/10.1016/j.biotechadv.2014.04.004 (2014).

20. Marques Almeida, A. et al. Curcumin and Capsaicin: From Spices to Cancer-Suppressing Agents. *RECIMA21 – Rev. Cient. Multidiscip* (2021).
21. Mondal, A. et al. Capsaicin and Its Nanoformulations as Anticancer Agents: A Comprehensive Review. *Phytother Res.* **38**, 1191–1223. https://doi.org/10.1002/ptr.8108 (2024).
22. Yip, K. W. & Reed, J. C. Bcl-2 Family Proteins and Cancer. *Oncogene* **27**, 6398–6406. https://doi.org/10.1038/onc.2008.307 (2008).
23. Davis, M. A., Turner, R. J. & Smith, P. Regulation of Apoptotic Pathways by Bcl-2 Family Proteins. *Biochem. J.* **475**, 2121–2135. https://doi.org/10.1042/BCJ20170726 (2018).
24. Moawad, M., Nasr, G. M., Osman, A. S. & Shaker, E. S. Gene Expression of Apoptosis-Related Proteins in HepG2 Cells Treated with Natural Compounds. *Int. J. Immunopathol. Pharmacol.* **37**, 1–11. https://doi.org/10.1177/20587384231128411 (2023).
25. Snyder, L. R., Kirkland, J. J. & Dolan, J. W. *Introduction to Modern Liquid Chromatography* (Wiley, 2011). https://doi.org/10.1002/9781118213617
26. Swartz, M. E. & Krull, I. S. *Handbook of Analytical Validation* (CRC, 2012). https://doi.org/10.1201/b12148
27. Petrakis, E. A. & Polissiou, M. G. Recent Advances in Chromatographic Methods for Bioactive Compounds in Spices. *TrAC Trends Anal. Chem.* **91**, 85–97. https://doi.org/10.1016/j.trac.2017.03.012 (2017).
28. Barbero, G. F., Palma, M. & Barroso, C. G. Determination of Capsaicinoids in Peppers by Liquid Chromatography–Electrospray–Mass Spectrometry. *Anal. Chim. Acta*. **586**, 227–233. https://doi.org/10.1016/j.aca.2007.12.024 (2008).
29. Li, S. et al. Chemical Composition and Product Quality Control of Turmeric (Curcuma longa L). *Pharm. Crops*. **2**, 28–54. https://doi.org/10.2174/2210290601102010028 (2011).
30. International Conference on Harmonisation (ICH). Validation of Analytical Procedures: Text and Methodology Q2(R1). Geneva. (2005). https://database.ich.org/sites/default/files/Q2%28R1%29%20Guideline.pdf
31. Yallapu, M. M., Jaggi, M. & Chauhan, S. C. Curcumin Nanoparticles: A Promising Nanomedicine for Cancer Therapy. *Drug Discov Today*. **17**, 71–80. https://doi.org/10.1016/j.drudis.2011.09.009 (2012).
32. Sharma, A., Arora, R. & Gupta, C. Advances in Nanodelivery of Curcumin for Cancer and Inflammatory Disorders. *Curr. Pharm. Des.* **26**, 3277–3290. https://doi.org/10.2174/1381612826666200320160110 (2020).
33. Meng, F. et al. Design and Evaluation of Curcumin-Loaded Lipid-Polymer Hybrid Nanoparticles for Improved Bioavailability. *Colloids Surf. B Biointerfaces*. **181**, 712–722. https://doi.org/10.1016/j.colsurfb.2019.06.017 (2019).
34. Bhushani, J. A., Singh, M. K., Sharma, S. & Sharma, M. Development and Characterization of Curcumin-Loaded Nanoliposomes for Food Applications. *J. Nanomater*. https://doi.org/10.1155/2016/5246028 (2016). Article ID 5246028.

35. Shaimaa, M. S., Nasser, M. A., Khaled, M. A. & Ahmed, A. A. *Capsaicin-Loaded Nanoliposomes: Preparation, Characterization, and Cytotoxic Evaluation. Nanomedicine 14*, 885–894. (2019). https://doi.org/10.2217/nnm-2018-0387
36. Kallifatidis, G. et al. The Role of Curcumin in Cancer Stem Cell Signaling and Chemoresistance. *Anticancer Res.* **28**, 437–445. https://doi.org/10.21873/anticanres.2915 (2008).
37. Salehi, B. et al. Pharmacological and Therapeutic Potential of Capsaicin and Its Nanoformulations: A Comprehensive Review. *Food Funct.* **10**, 5393–5410. https://doi.org/10.1039/c9fo01234a (2019).
38. Vaz, G. R. et al. Curcumin and Quercetin-Loaded Nanoemulsions: Physicochemical Compatibility Study and Validation of a Simultaneous Quantification Method. *Nanomaterials 10* (9), 1650. (2020). https://doi.org/10.3390/nano10091650
39. Chen, X. et al. Sustained Release, and Cellular Antioxidant Activity of Curcumin Nanoliposomes. *Molecules* **20** (8), 14293–14311. https://doi.org/10.3390/molecules200814293 (2015).
40. Danaei, M. et al. Impact of Particle Size and Polydispersity Index on the Clinical Applications of Lipidic Nanocarrier Systems. *Pharmaceutics 10* (2), 57. (2018). https://doi.org/10.3390/pharmaceutics10020057
41. Zhang, S. & Wang, C. Precise Analysis of Nanoparticle Size Distribution in TEM Images. *Methods Protoc.* **6**, 63. https://doi.org/10.3390/mps6040063 (2023).
42. Ribeiro, L. N. M. et al. Liposomal Formulations for Improved Bioavailability of Phytochemicals. *Int. J. Pharm.* **494**, 121–132. https://doi.org/10.1016/j.ijpharm.2015.08.033 (2015).
43. Chaudhuri, P., Harfouche, R., Soni, S., Hentschel, D. M. & Sengupta, S. Nanocarrier-Mediated Combination Therapy for Cancer Treatment: The Future of Chemotherapy. *Adv. Drug Deliv Rev.* **62**, 342–351. https://doi.org/10.1016/j.addr.2009.11.021 (2010).
44. Mozafari, M. R. Liposomes: An Overview of Manufacturing Techniques. *Cell. Mol. Biol. Lett.* **10** (4), 711–719 (2005). PMID: 16341210.
45. Pecora, R. *Dynamic Light Scattering: Applications of Photon Correlation Spectroscopy* (Plenum, 1985).
46. International Organization for Standardization. *ISO 13321: Methods for Determination of Particle Size Distribution—Part 8: Photon Correlation Spectroscopy* Vol. (Geneva, 1996).
47. Liu, F. et al. Curcumin-Induced Autophagy Anticancer Effects on Human Lung Adenocarcinoma Cell Line A549. *Oncol. Lett.* **14** (3), 2775–2782. https://doi.org/10.3892/ol.2017.6565 (2017).
48. Ziasarabi, P., Sahebkar, A. & Ghasemi, F. Evaluation of the Effects of Nanomicellar Curcumin, Berberine, and Their Combination with 5-Fluorouracil on Breast Cancer Cells. In *Natural Products and Human Diseases*; Sahebkar, A.; Sathyapalan, T., Eds.; *Advances in Experimental Medicine and Biology*; Springer: Cham, ; Vol. 1328, pp 29–42. (2021). https://doi.org/10.1007/978-3-030-73234-9_3
49. Vogelstein, B., Lane, D. & Levine, A. J. Surfing the p53 Network. *Nat. Med.* **6**, 693–698. https://doi.org/10.1038/75127 (2000).

50. Youle, R. J. & Strasser, A. The BCL-2 Protein Family: Opposing Activities That Mediate Cell Death. *Nat. Rev. Mol. Cell. Biol.* **9**, 47–59. https://doi.org/10.1038/nrm2308 (2008).
51. Chong, S. J. F. et al. Mechanistic Insights into Apoptosis Pathways Modulated by Nano-Curcumin and Nano-Capsaicin. *Mol. Cancer*. **24**, 62. https://doi.org/10.1186/s12943-025-02135-4 (2025).
52. Zhang, Y. et al. 53-Dependent Induction of Apoptosis by Natural Compounds in Cancer Cells. *Oncogene* **23**, 6114–6122. https://doi.org/10.1038/sj.onc.1207770 (2004).
53. Levine, A. J. *p53, the Cellular Gatekeeper for Growth and Division. Cell 88*, 323–331. (1997). https://doi.org/10.1016/S0092-8674(00)81871-1
54. Vousden, K. H. & Lu, X. Live or Let Die: The Cell's Response to p53. *Nat. Rev. Cancer*. **2**, 594–604. https://doi.org/10.1038/nrc864 (2002).
55. Chen, Y. et al. Synergistic Effects of Curcumin and Capsaicin in Cancer Cells. *Mol. Carcinog.* **48** (9), 885–896. https://doi.org/10.1002/mc.20527 (2009).
56. Suresh, D., Srinivasan, K., Sambandam, N. & Sankar, R. Curcumin and Capsaicin Combinations Exhibit Synergistic Anti-Cancer Effects through Induction of Apoptosis in Human Liver Cancer Cells. *Cancer Cell. Int.* **19**, 235. https://doi.org/10.1186/s12935-019-0961-6 (2019).
57. Putri, G. F. T. & Nurfatihah, Z. Z. Bax/Bcl-2 Ratio as the Golden Marker of Apoptosis: Molecular Mechanisms and Regulatory Pathways. *Int. J. Cell. Biomed. Sci.*, **4** (10), 309–317. https://doi.org/10.59278/cbs.v4i10.65. (2025).
58. Xu, J., Ji, L. & Xu, L. Lead-Induced Apoptosis in PC12 Cells: Involvement of p53, Bcl-2 Family and Caspase-3. *Toxicol. Lett.*, **166** (2), 160–167. (2006).
59. Liu, L., Sun, M., Wang, Y. & Zhang, Y. Gene Expression Profiles of Bax, Bcl-2, and p53 in Human Liver Cancer. *Cancer Res.* **58** (7), 1463–1468 (1998). PMID: 9537240.
60. Jiang, P., Du, W., Heese, K. & Wu, M. The Bad, the Good and the Ugly: The Roles of Bcl-2 Family Proteins in Apoptosis. *Cell. Cycle*. **8**, 844–852. https://doi.org/10.4161/cc.8.6.8043 (2009).
61. Ashkenazi, A. & Dixit, V. M. Apoptosis Control by Death and Decoy Receptors. *Curr. Opin. Cell. Biol.* **11** (2), 255–260. https://doi.org/10.1016/S0955-0674(99)80034-9 (1999).
62. Smith, P., Davis, M. A. & Turner, R. J. HPLC Determination of Capsaicinoids in Chili Peppers. *Food Chem.* **318**, 126458. https://doi.org/10.1016/j.foodchem.2020.126458 (2020).
63. Brown, K., Green, T. & White, J. H. P. L. C. Determination of Capsaicinoids in Chili Peppers. *Food Chem.* **280**, 243–251. https://doi.org/10.1016/j.foodchem.2018.12.015 (2019).
64. Lee, M., Kim, S. & Park, J. H. P. L. C. Analysis of Curcumin in Turmeric Extracts. *J. Agric. Food Chem.* **69** (25), 7534–7542. https://doi.org/10.1021/acs.jafc.1c02039 (2021).
65. Patel, H. & Kumar, N. Extraction and Quantification of Curcumin from Turmeric. *J. Food Sci.* **87** (4), 1189–1198. https://doi.org/10.1111/1750-3841.16047 (2022).
66. Bangham, A. D., Standish, M. M. & Watkins, J. C. Diffusion of Univalent Ions across the Lamellae of Swollen Phospholipids. *J. Mol. Biol.* **13** (1), 238–252. https://doi.org/10.1016/S0022-2836(65)80093-6 (1965).

67. Zhao, X. & Wang, Y. T. E. M. Analysis of Lipid Nanoparticles. *Microsc Res. Tech.* **81** (9), 921–928. https://doi.org/10.1002/jemt.23055 (2018).
68. Kumar, P. & Singh, R. Nanoparticle Characterization Using DLS and Zeta Potential Measurements. *Nanotechnology* **31** (26), 265102. https://doi.org/10.1088/1361-6528/ab7d6b (2020).
69. Thomas, S., Kumar, R., Singh, N., Gupta, R. & Sharma, R. Fourier Transform Infrared Spectroscopy Analysis of Liposomal Nanoparticles. *Spectrochim Acta Mol. Biomol. Spectrosc.* **223**, 117318. https://doi.org/10.1016/j.saa.2019.117318 (2019).
70. Wang, X. et al. Thermal Characterization of Nanocarriers Using DSC. *Thermochim Acta*. **683**, 178455. https://doi.org/10.1016/j.tca.2019.178455 (2020).
71. Zhang, X. et al. Evaluation of the Anticancer Activity of Curcumin Nanoparticles. *Biomed. Pharmacother*. **133**, 111038. https://doi.org/10.1016/j.biopha.2020.111038 (2021).
72. Schroeder, A. et al. The RNA Integrity Number: A New Standard for RNA Quality Assessment. *Nat. Methods*. **3** (6), 41–46. https://doi.org/10.1038/nmeth893 (2006).
73. Imbeaud, S. et al. Towards Standardization of RNA Quality Assessment Using Degradation Signatures. *Biotechnol. Appl. Biochem.* **40** (3), 249–259. https://doi.org/10.1042/BA20040118 (2005).
74. Bustin, S. A. et al. The MIQE Guidelines: Minimum Information for Publication of Quantitative Real-Time PCR Experiments. *Clin. Chem.* **55** (4), 611–622. https://doi.org/10.1373/clinchem.2008.112797 (2009).
75. Livak, K. J. & Schmittgen, T. D. Analysis of Relative Gene Expression Data Using Real-Time Quantitative PCR and the 2^−ΔΔCt Method. *Methods* **25** (4), 402–408. https://doi.org/10.1006/meth.2001.1262 (2001).
76. Vandesompele, J. et al. Accurate Normalization of Real-Time Quantitative RT-PCR Data by Geometric Averaging of Multiple Internal Control Genes. *Genome Biol.* **3** (7). https://doi.org/10.1186/gb-2002-3-7-research0034 (2002). research0034.1.

Figures

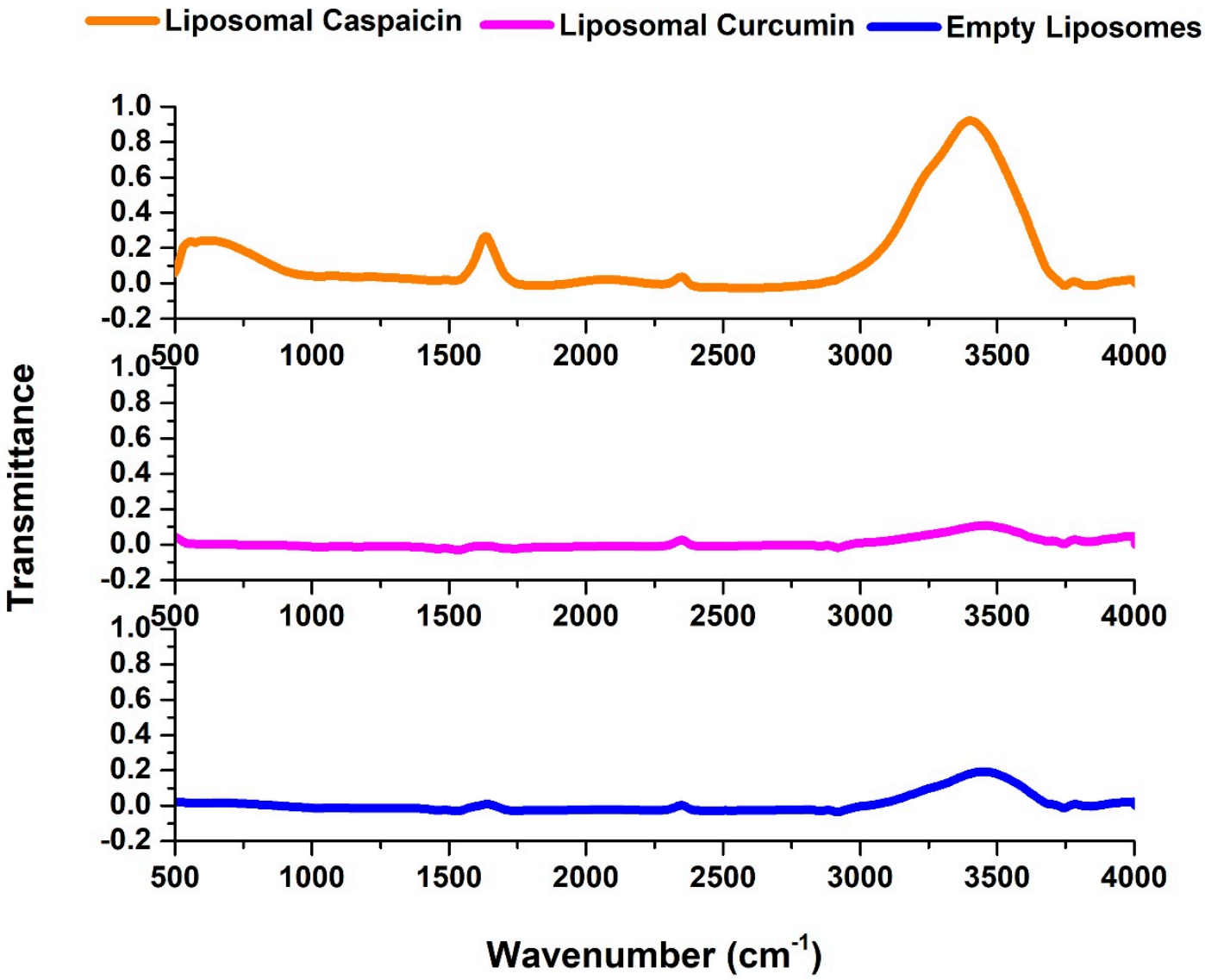


Figure 1

The full FTIR spectra of empty lecithin and lecithin / Curcumin or Capsaicin liposomal samples.

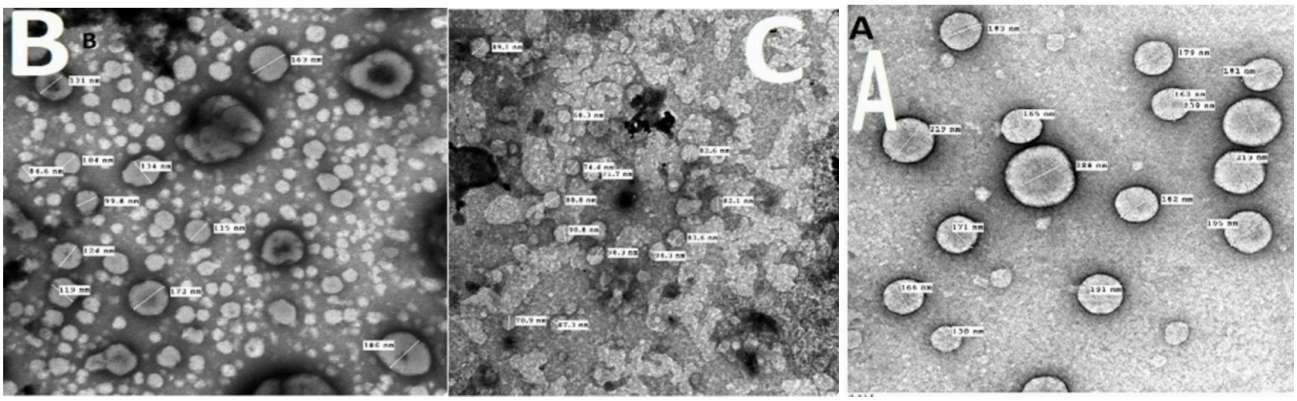


Figure 2

TEM images for controlliposomes (A), Curcumin-loaded liposomes (B) and Capsaicin-loaded liposomes (C).

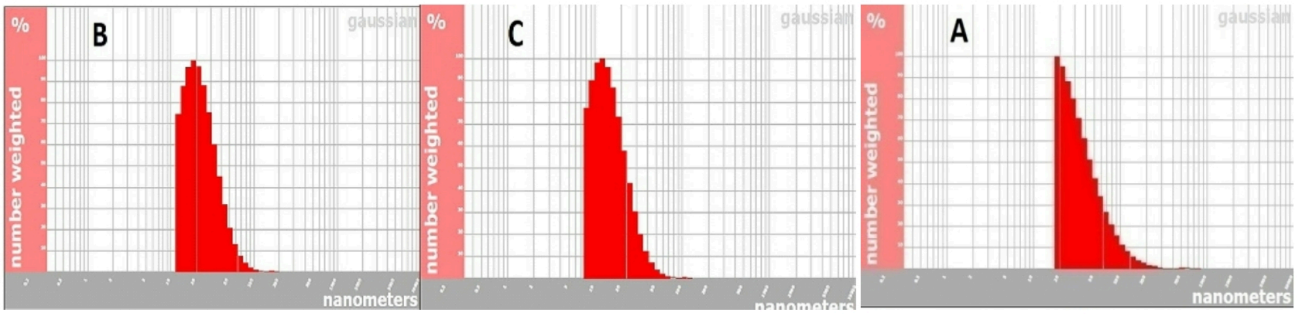


Figure 3

Particle Size distribution of liposomes analyzed by dynamic light scattering (DLS) for (A) empty lecithin liposomal sample, (B) Curcumin-encapsulated liposomes and (C) Capsaicin-encapsulated liposomes.

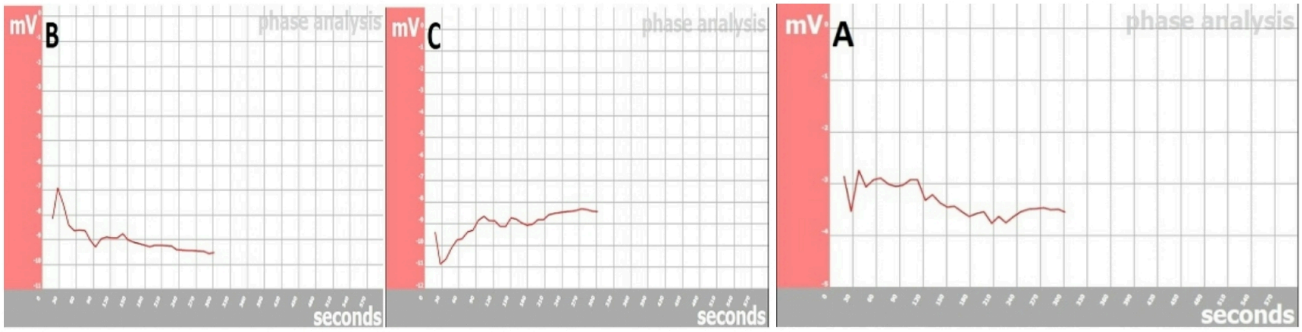


Figure 4

Zeta potential for (A) empty lecithin liposomal sample, (B) Curcumin-encapsulated liposomes and (C) Capsaicin-encapsulated liposomes.

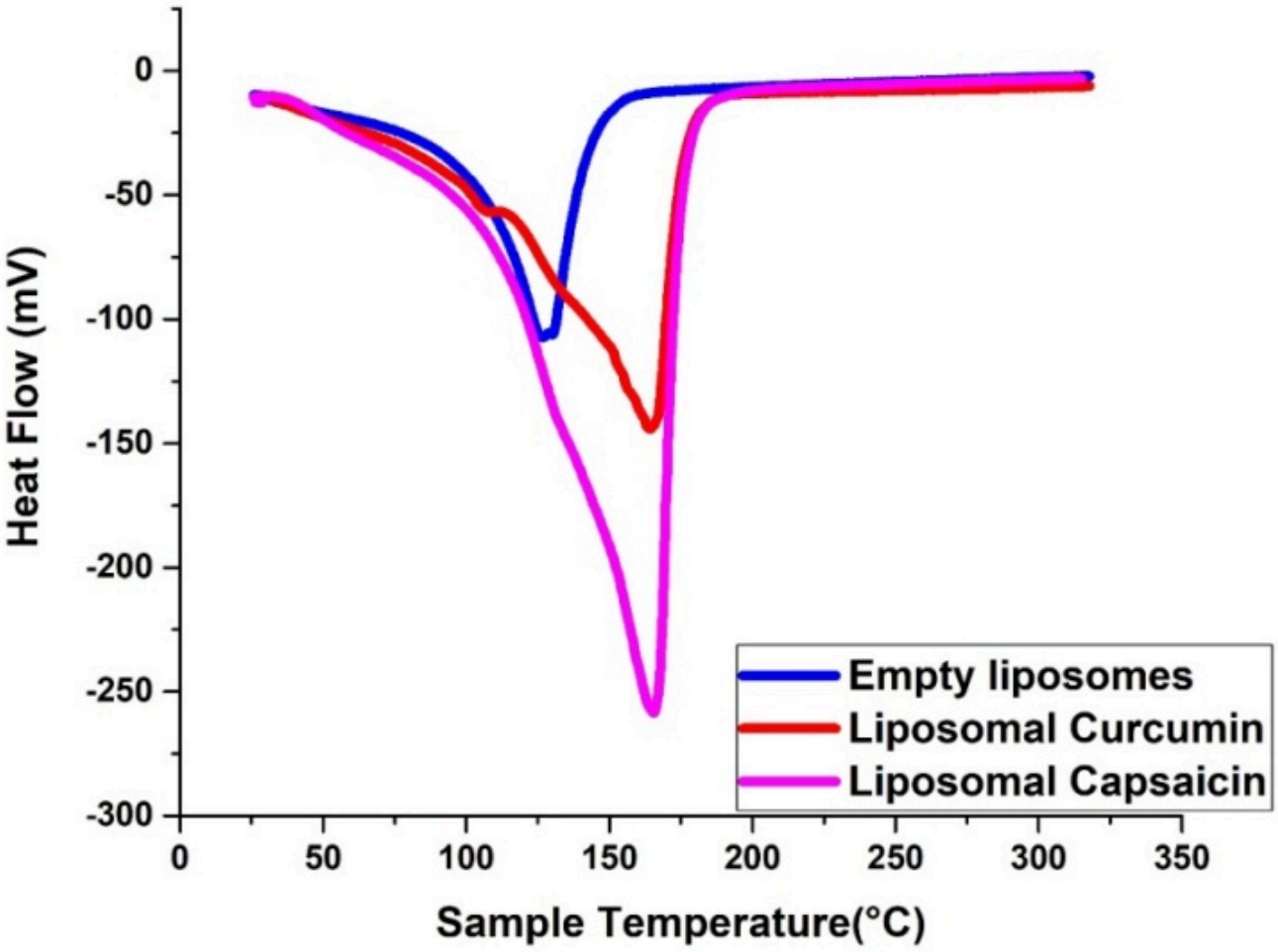


Figure 5

DSC curves for pure lecithin, liposomes doped with either Curcumin or Capsaicin.

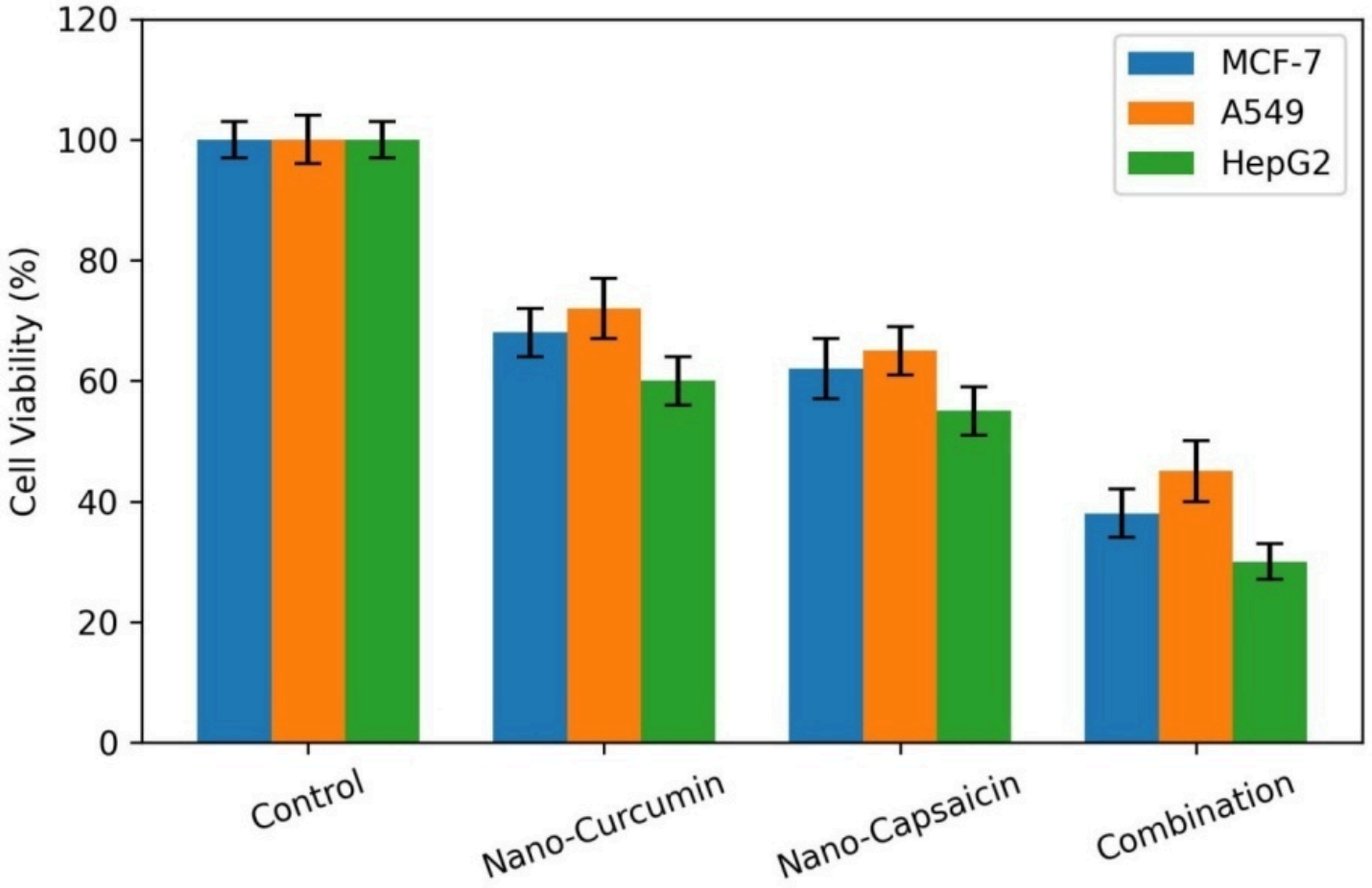


Figure 6

Cell viability assessed by MTT assay following treatment with individual and combined nano-formulations (Nano-Curcumin, Nano-Capsaicin, and their combination) in MCF-7, A549, and HepG2 cells. Results are expressed as percentage cell viability relative to untreated control cells and presented as mean ± SD.

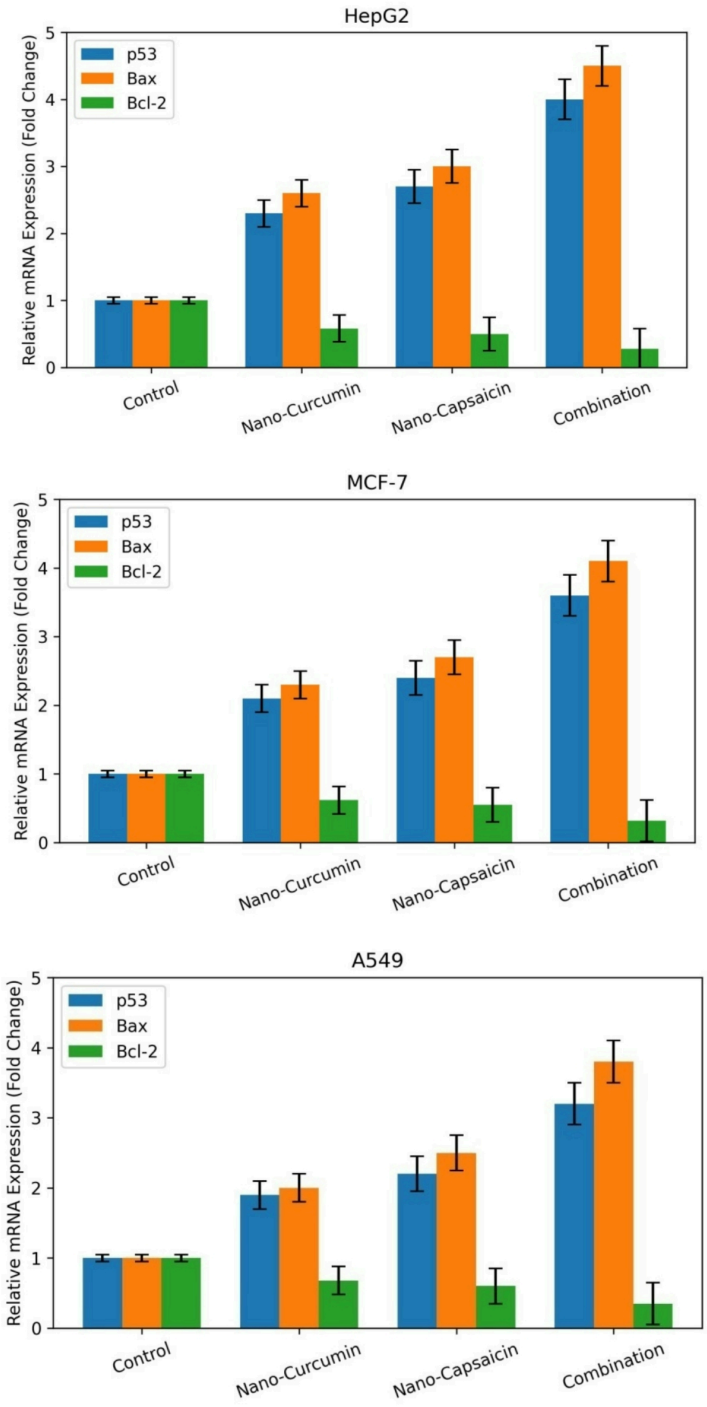


Figure 7

Relative mRNA expression levels of pro-apoptotic genes (p53 and Bax) and the anti-apoptotic gene (Bcl-2) in MCF-7, A549, and HepG2 cells treated with Nano-Curcumin, Nano-Capsaicin, and their combination, as measured by quantitative RT-PCR. Data are expressed as fold change relative to control cells and presented as mean ± SD.

Supplementary Files

This is a list of supplementary files associated with this preprint. Click to download.

- floatimage1.png
- floatimage2.jpeg